Available online at www.sciencedirect.com
SCIENCE DIRECT®
International Journal of Mass Spectrometry 226 (2003) 317–327
International Journal of Mass Spectrometry
www.elsevier.com/locate/ijms

Molecular and dissociative photoionization of CS_2 from 20 to 120 eV

Toshio Masuoka*, Atsuo Okaji, Ataru Kobayashi

Department of Applied Physics, Graduate School of Engineering, Osaka City University, Sugimoto 3-3-138, Sumiyoshi-ku, Osaka 558-8585, Japan

Received 20 December 2002; accepted 23 January 2003

Abstract

Using synchrotron radiation as a continuum light source, molecular and dissociative photoionization of CS_2 has been studied in the photon-energy region of 20–120 eV. Ion branching ratios obtained by analyzing the time-of-flight (TOF) mass spectra for the observed ions, S_2^+, CS^+, S^+, C^+, and CS_2^{2+}, were differentiated with respect to the incident photon energy. The results obtained by this analytical photoion spectroscopy show dissociation pathways of the parent CS_2^+ and CS_2^{2+} ions, some of which are observed for the first time in the present study. These pathways are discussed by comparing them with the reported electronic states of the ions.

Keywords: Dissociative photoionization; Carbon disulfide; Ion branching ratios; Synchrotron radiation

1. Introduction

Many mass spectrometric experiments have been carried out to study formation and dissociation mechanisms of singly, doubly, and triply charged molecular cations of CS_2. The studies for these cations reported prior to 1989 were reviewed by Mathur and Harris [1]. After this review, many researches have been reported on CS_2 including the studies of complete valence shell photoelectron spectrum [2], dissociative ionization by photoelectron–photoion coincidence (PEPICO) spectroscopy [3], double photoionization by photoelectron–photoelectron coincidence (PEPECO) and PEPICO spectroscopy [4], by a threshold photoelectrons coincidence (TPEsCO) method [5], by PEPICO and photoelectron–photoion–photoion coincidence (PEPIPICO) experiments [6], by a position sensitive PEPIPICO method [7], and by theoretical calculations [8].

The electron configuration of CS_2 in the ground electronic state is

$$(\text{core})(5\sigma_g^2 4\sigma_u^2)(6\sigma_g^2 5\sigma_u^2 2\pi_u^4 2\pi_g^4);\ ^1\Sigma_g^+.$$

The most recently examined photoelectron spectrum of CS_2 reported by Baltzer et al. [2] shows very rich and strong satellite states as well as single-hole states arising from the four outer valence orbitals. Their photoelectron spectrum recorded with synchrotron radiation demonstrates that the inner valence region contains a much complicated structure due to the

* Corresponding author. Tel.: +81-66-605-2879; fax: +81-66-605-2769.
E-mail address: masuoka@a-phys.eng.osaka-cu.ac.jp (T. Masuoka).

1387-3806/03/$ – see front matter © 2003 Elsevier Science B.V. All rights reserved.
doi:10.1016/S1387-3806(03)00025-3

multielectron processes, and that distinct features are discernible up to a binding energy of at least 34 eV. A comparison of the experimental peaks with satellite states predicted from the Green's function calculations [2] displays a complete breakdown of the single particle model of ionization for the $5\sigma_g$ and $4\sigma_u$ inner valence orbitals. No main line can be distinguished for either orbital. Recently, Aitchison and Eland [3] have examined dissociative ionization of CS_2 from the electronic states of CS_2^+ up to 27 eV, including the satellite bands 3, 4, 6, and 10, using PEPICO spectroscopy and have given the branching ratios to the ions S^+, CS^+, S_2^+, and C^+. They also deduced kinetic energy release distributions from the peak shape and inferred the states of the fragmentations. However, the dissociation of high-lying satellite bands has not been studied yet, therefore, it remains as an open question.

As for double photoionization, the most reliable threshold reported so far lies at 27.05 ± 0.02 eV measured by TPEsCO spectroscopy [5]. The removal of two electrons from the outermost orbital yields a metastable CS_2^{2+} ion in the $X^3\Sigma_g^-$ ground and the $a^1\Delta_g$ and $b^1\Sigma_g^+$ excited electronic states [5,9]. The cross section for the formation of metastable CS_2^{2+} by photoionization has been reported from the threshold up to 50 eV [9,10]. In addition to CS_2^{2+}, Lablanquie et al. [9] studied dissociative double photoionization and reported the cross sections as well as the thresholds for three dissociation channels, $S^+ + CS^+$, $S^+ + C + S^+$, and $S^+ + C^+ + S$. However, it has not been clearly determined which dissociation channel is effectively open at what energy region, which also remains as an open question.

In this paper, ion branching ratios for the molecular and dissociative ionization of CS_2 are presented from 20 to 120 eV. The observed ion branching ratios were differentiated with respect to the incident photon energy. The results obtained by this analytical photoion spectroscopy show dissociation pathways of the parent CS_2^+ and CS_2^{2+} ions. That is, this spectroscopy provides a method to better visualize the opening of the new dissociation channels. These pathways are discussed by comparing them with the reported electronic states of the ions. The present results shed light on the open questions mentioned above.

2. Experiment

A time-of-flight (TOF) mass spectrometer [11,12] was used to measure photoionization mass spectra at the Ultraviolet Synchrotron Orbital Radiation (UVSOR) facility of the Institute for Molecular Science (IMS) in the 20–120 eV region with Sn (20–36 eV) and Al (37–70 eV) optical filters (no filter above 72.5 eV) for higher order radiation sorting. The sample gas was introduced in the ionization region by an effusive jet. The TOF mass spectra were measured at an angle of $\sim 55^\circ$ with respect to the plane of the storage ring to minimize the effects of anisotropic angular distributions of fragment ions [13] with 1, 2, and 2.5 eV intervals in the energy regions of 20–50, 50–70, and 70–120 eV, respectively. A relatively high electric field (2250 V/cm) was applied to the ionization region to minimize discrimination effects against energetic ions, particularly produced by dissociative double photoionization. The impinging energy of the ions on the microchannel plate (MCP) detector was $\sim$3.9 keV. The TOF mass spectrometer was operated in two modes [14]. In mode A, the photoelectron signal was used as a start pulse of a time-to-amplitude converter (TAC). In this mode, the relative ion yields in single and double photoionization were not properly evaluated mainly because of the different number of photoelectrons in the two processes. The number of ions produced in double photoionization was overestimated because the probability of forming one output pulse from a channel electron multiplier (CEM) is higher for two electrons hitting simultaneously than for one electron. This mode was used to check the type of ions produced particularly at higher photon energies. This problem was overcome by using the radio frequency (rf) signal (90.115 MHz) of the storage ring operated in a single-bunch mode (the time between adjacent photon bunches is 177.6 ns) as the start pulse of the TAC by reducing the frequency appropriately (mode B). In this mode, it is believed that

the observed mass spectra are free from the discrimination between single and double photoionization because the Ar^{2+}/Ar^{+} ratio measured in the region from the double photoionization threshold to 100 eV was in good agreement with previous reports [15]. The Ar^{2+}/Ar^{+} ratio has been reported to be very dependent on gas pressure and discriminator setting [16,17]. In this experiment, since the gas pressure in the TOF mass spectrometer was $\sim 2.5 \times 10^{-7}$ Torr and the MCP detector was used at the middle of a counting plateau, we believe that the Ar^{2+}/Ar^{+} ratio is reliable. The statistical accuracy of the signals was typically better than 1% for the major ions. The band pass of the monochromator was 0.4 Å (80–120 eV), 0.8 Å (37–77.5 eV) and 2.4 Å (20–36 eV), which means the worst band pass was 0.46 eV at 120 eV. $E/\Delta E$ was in the range of 145 (36 eV)–420 (37 eV). An estimate of the total uncertainty in the data is less than ±15%.

The dissociation processes observed by the present TOF mass spectra and PIPICO spectra [9] are as follows:In these processes, autoionization of super

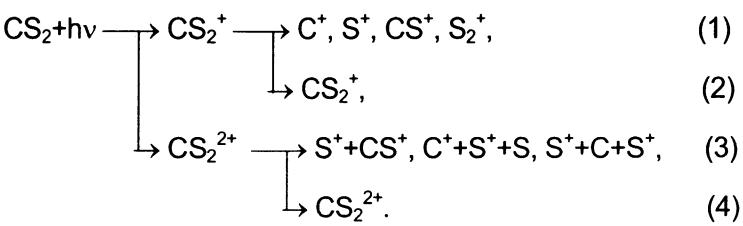

excited CS_2^{*}, CS_2^{**}, and CS_2^{+*} is not explicitly presented. Only the final dissociation products in a microsecond time scale are indicated for simplicity. The experimental quantity to be measured is the ion branching ratios for the ions produced in the processes given in Eqs. (1)–(4). When dissociative double photoionization occurs (Eq. (3)), the heavier ion is not counted in the TOF mass spectra if the ion-detection efficiency is high. This is because the lighter ion stops the TAC. Since the ion-detection efficiency of the MCP used at UVSOR was of the order of a few percent, the heavier ions were detected with almost the same efficiency as the lighter ions. The low ion detection efficiency of the MCP is partly due to an aging effect caused by using the same detector for a long period of time and partly due to not using a mesh in front of the MCP which is usually used to produce a retarding field for photoelectrons ejected to the opposite side of the ion detector. Even though the ion-detection efficiency of the MCP is low, it should be noted that this does not affect the quality of the mass spectra [18]. Instead, it only increases the accumulation time of the spectra to attain necessary counting statistics. Although PIPICO spectra have also been measured by our group, the results will be reported separately.

3. Results and discussion

The ion branching ratios are shown in Fig. 1 together with those of Carnovale et al. [10] for comparison. The numerical values are given in Table 1. Carnovale et al. [10] have studied the fragmentation of CS_2 using pseudo-photon (electron energy-loss) techniques and obtained branching ratios of the ions indicated in Fig. 1 from 13 to 40 eV. The authors make suggestions as to how the ground and excited states of CS_2^{+} (X, A, B, C, and satellite states) are related to the production of the ionic fragments. For example, they suggest that the C state dissociates into CS^{+} and S^{+} in a 60:40 ratio, which is in agreement with the results of Brehm et al. [19]. It can be seen in Fig. 1 that the overall agreement between the two data sets is very good. Some noticeable discrepancy can be seen in the branching ratios of CS^{+} around 25 eV. The reason for this is not clear at present. Since reliable total absorption cross sections have not been reported for CS_2 in the wide energy region, the partial photoionization cross sections for the product ions cannot be

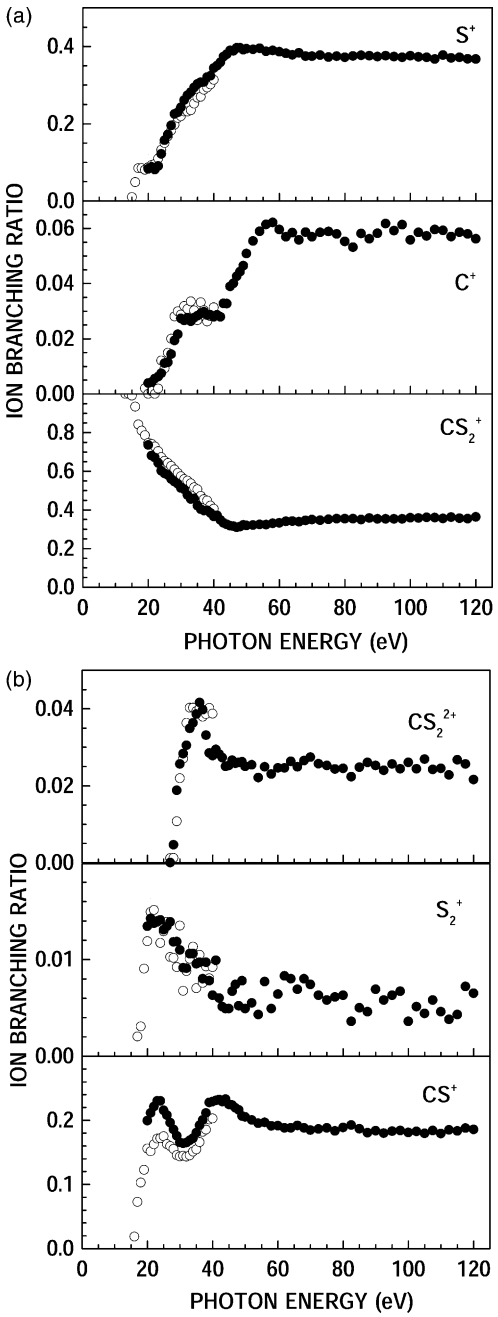

Fig. 1. Ion branching ratios of CS_2: (●), present data; (○), from [10].

obtained. As can be seen in Fig. 1, the ion branching ratios for the C^+, S^+, CS^+, S_2^+, and CS_2^{2+} ions show sharp increases at various photon energies. These increases in the branching-ratio curves relate to the opening of the corresponding dissociation channels. In order to correlate these dissociation pathways more clearly to the electronic states of CS_2^+ and CS_2^{2+}, the ion branching ratios for these ions were differentiated with respect to the photon energy. This differential spectroscopy shows a clear correspondence between a certain dissociation channel and specific energy regions. This analytical photoion spectroscopy has been described previously [20,21] and further discussed in our recently reported studies of SO_2 [22] and CF_4 [18,23].

The resultant photoion spectra are shown in Figs. 2–6 with solid circles and thick solid curves, in which the positive peaks indicate the dissociation pathways of CS_2^+, CS_2^*, CS_2^{**}, CS_2^{+*}, and CS_2^{2+} to the respective ions. The negative peaks indicate simply that the ion branching ratio for a given fragment decreases as the incident photon energy increases because of a decrease of the ion branching ratio for the given fragment or an increase of the ion branching ratio for some other fragment(s). The differential spectra derived from the data [10] are also shown in these figures with open circles and thin solid curves. Their data have been measured at an interval of 1 eV with the energy resolution of about 1 eV FWHM. The differential spectra shown with circles were obtained by the use of Origin (Microcal), in which the derivative was taken by averaging the slopes of the two adjacent pairs of the data points. Note that this treatment causes a spectral broadening of the order of the interval between two adjacent data points. The solid curves in Figs. 2–6 are the results of a least-squares fit to the derivatives by a *B*-spline function by using Origin. As for the error margins in the differential spectra, one may evaluate the magnitude from the scattering of the derivatives at high energies where the spectra are essentially flat. However, it is difficult to generalize the error margins at energies near the thresholds.

Table 1
Ion branching ratios for the fragmentation of CS_2

Photon energy (eV)	C^+	S^+	CS_2^{2+}	CS^+	S_2^+	CS_2^+
20.0	0.0039	0.083		0.199	0.013	0.735
21.0	0.0042	0.088		0.211	0.014	0.681
22.0	0.0055	0.081		0.221	0.014	0.670
23.0	0.0062	0.090		0.230	0.014	0.642
24.0	0.0074	0.122		0.230	0.014	0.602
25.0	0.011	0.157		0.216	0.013	0.587
26.0	0.011	0.172		0.208	0.013	0.580
27.0	0.014	0.195	0	0.196	0.014	0.560
28.0	0.019	0.225	0.0046	0.186	0.012	0.546
29.0	0.022	0.229	0.019	0.176	0.012	0.535
30.0	0.027	0.242	0.026	0.165	0.011	0.513
31.0	0.027	0.261	0.028	0.164	0.0091	0.506
32.0	0.028	0.274	0.031	0.165	0.0091	0.476
33.0	0.026	0.281	0.035	0.168	0.011	0.456
34.0	0.028	0.293	0.036	0.172	0.011	0.458
35.0	0.028	0.303	0.039	0.180	0.0096	0.421
36.0	0.029	0.307	0.042	0.192	0.0097	0.403
37.0	0.030	0.308	0.040	0.200	0.0080	0.396
38.0	0.029	0.320	0.033	0.211	0.0097	0.397
39.0	0.029	0.324	0.029	0.228	0.0078	0.383
40.0	0.028	0.343	0.028	0.229	0.0063	0.366
41.0	0.029	0.350	0.029	0.231	0.0099	0.371
42.0	0.028	0.359	0.028	0.232	0.0060	0.347
43.0	0.033	0.373	0.027	0.229	0.0051	0.332
44.0	0.033	0.380	0.025	0.233	0.0049	0.325
45.0	0.039	0.389	0.025	0.225	0.0049	0.317
46.0	0.040	0.388	0.027	0.224	0.0067	0.315
47.0	0.043	0.396	0.026	0.219	0.0074	0.309
48.0	0.044	0.396	0.026	0.216	0.0052	0.312
49.0	0.046	0.391	0.026	0.207	0.0078	0.322
50.0	0.051	0.394	0.025	0.205	0.0049	0.318
52.0	0.055	0.392	0.025	0.200	0.0055	0.321
54.0	0.059	0.395	0.022	0.195	0.0043	0.325
56.0	0.061	0.387	0.025	0.197	0.0077	0.323
58.0	0.062	0.389	0.023	0.191	0.0049	0.330
60.0	0.060	0.386	0.025	0.191	0.0064	0.333
62.0	0.057	0.382	0.025	0.188	0.0083	0.340
64.0	0.058	0.378	0.026	0.188	0.0080	0.342
66.0	0.056	0.383	0.025	0.192	0.0069	0.338
68.0	0.059	0.374	0.027	0.188	0.0080	0.345
70.0	0.057	0.375	0.027	0.185	0.0074	0.349
72.5	0.059	0.377	0.026	0.186	0.0063	0.346
75.0	0.059	0.372	0.025	0.188	0.0058	0.350
77.5	0.058	0.374	0.024	0.183	0.0061	0.354
80.0	0.055	0.372	0.025	0.189	0.0063	0.354
82.5	0.053	0.375	0.022	0.192	0.0036	0.354
85.0	0.058	0.377	0.025	0.187	0.0050	0.349
87.5	0.056	0.375	0.026	0.180	0.0046	0.358
90.0	0.058	0.373	0.025	0.184	0.0069	0.353
92.5	0.062	0.376	0.024	0.180	0.0058	0.353
95.0	0.059	0.373	0.026	0.183	0.0063	0.353
97.5	0.061	0.371	0.024	0.184	0.0067	0.352

Table 1 (*Continued*)

Photon energy (eV)	C^+	S^+	CS_2^{2+}	CS^+	S_2^+	CS_2^+
100.0	0.056	0.375	0.026	0.181	0.0036	0.359
102.5	0.059	0.373	0.024	0.183	0.0051	0.357
105.0	0.057	0.372	0.027	0.179	0.0044	0.360
107.5	0.060	0.367	0.024	0.184	0.0058	0.360
110.0	0.059	0.377	0.025	0.179	0.0046	0.355
112.5	0.057	0.370	0.023	0.185	0.0038	0.362
115.0	0.059	0.372	0.027	0.183	0.0043	0.356
117.5	0.058	0.368	0.026	0.188	0.0072	0.354
120.0	0.056	0.367	0.022	0.186	0.0065	0.363

3.1. The CS_2^+ ion

The ion branching ratio for the parent CS_2^+ ion (Fig. 1a) shows that the ratio decreases from low excitation energies up to 47 eV. However, the ratio increases slightly above 47 up to ~80 eV, which suggests that electronic states contributing to the production of the parent CS_2^+ ion exist in this energy region. This is somewhat surprising because electronic states lying in such a high energy region are usually thought to be all repulsive and/or to produce doubly charged ions. The existence of electronic states contributing to the production of singly charged parent ions in high energy regions has been observed for CO [14], CO_2 [24], and SO_2 [25]. In these cases, the ion branching ratios for the individual ions respectively produced from the parent m^+ and m^{2+} ions are determined separately at excitation energies where the molecular and dissociative single- and double-photoionization processes take place simultaneously.

With respect to the production of the parent CS_2^+ ion in the high energy region, three routes should be considered: (a) direct single ionization with another electron excited to a high-lying electronic state (CS_2^{+*}), which is a bound type and stable against dissociation in a microsecond time scale, (b) indirect

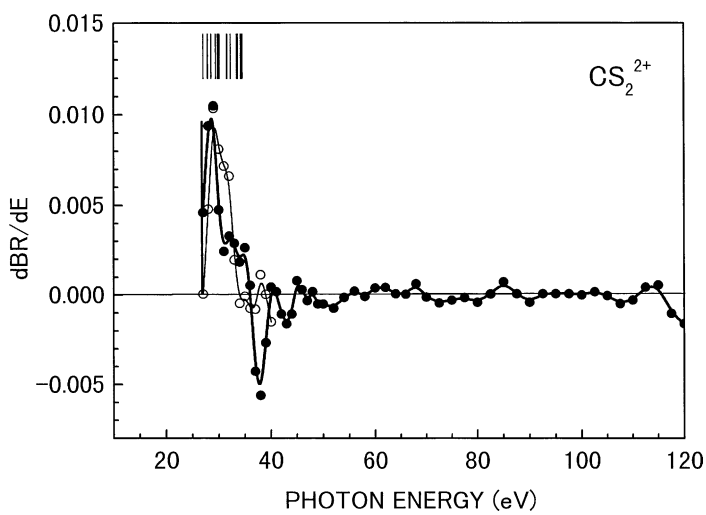

Fig. 2. Differential spectrum of ion branching ratio for CS_2^{2+}: (●) and thick solid curve, present data; (○) and thin solid curve, derived from [10].

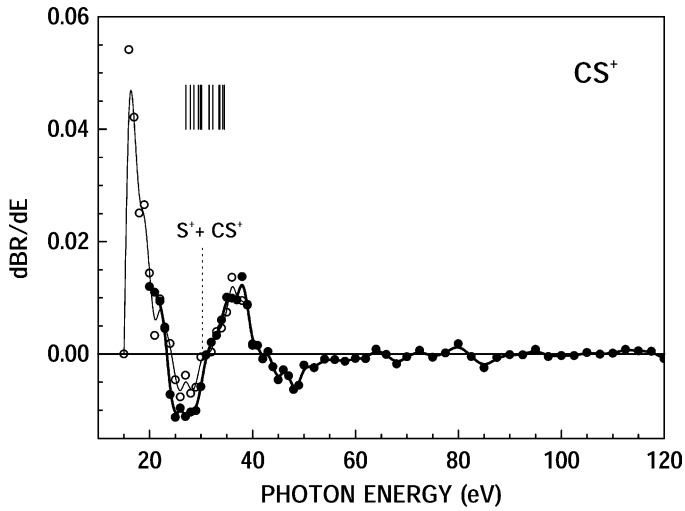

Fig. 3. Differential spectrum of ion branching ratio for CS^+: (●) and thick solid curve, present data; (○) and thin solid curve, derived from [10].

single ionization via resonant excitation to a double Rydberg state (CS_2^{**}) of the neutral, which autoionizes to a high-lying bound electronic state mentioned above, and (c) double Rydberg states autoionizing to the low-lying bound electronic states, such as $X^2\Pi_g$, $A^2\Pi_u$, and $B^2\Sigma_u^+$ states of CS_2^+; except for some possible contribution of three-hole-two-particle (CS_2^{+**}) and three-hole-three-particle (CS_2^{***}) excited configurations [26]. The last route (c) implies a two-electron transition in which one electron is removed and the other fills out a positive hole in a valence orbital like an Auger process. High-lying CS_2^{2+} states are all dissociative because of Coulomb repulsion. Higher members of the Rydberg states converging to these CS_2^{2+} states would also be dissociative because of a similarity of the ion core of the

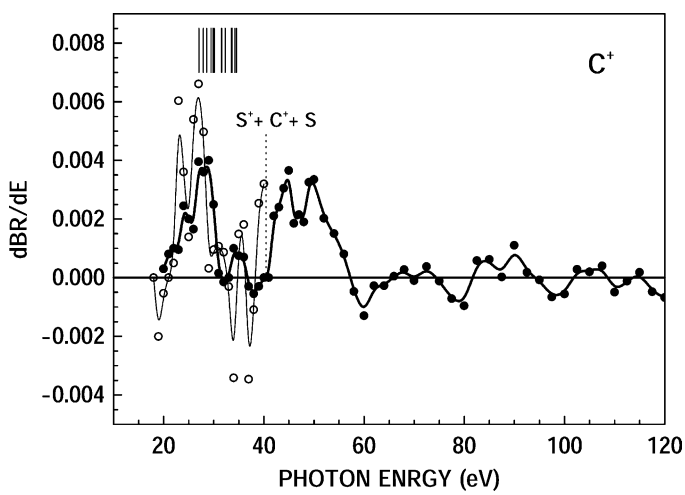

Fig. 4. Differential spectrum of ion branching ratio for C^+: (●) and thick solid curve, present data; (○) and thin solid curve, derived from [10].

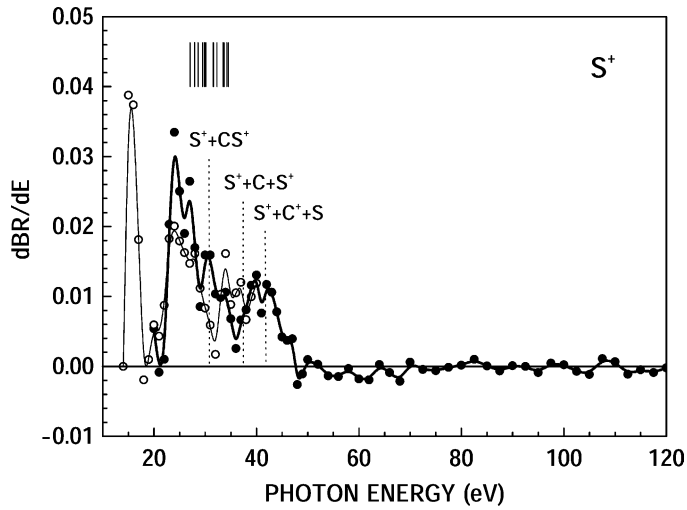

Fig. 5. Differential spectrum of ion branching ratio for S^+: (●) and thick solid curve, present data; (○) and thin solid curve, derived from [10].

Rydberg states with CS_2^{2+}. If this is the case, routes (a) and (b) would not be effective and route (c) would play an important role in the production of molecular CS_2^+ at higher excitation energies.

3.2. The CS_2^{2+} ion

The threshold for double photoionization reported by Hochlaf et al. [5] is indicated by a long vertical line in Fig. 2. Theoretical calculations of the energies of low-lying electronic states of the dication are available [8,26], of which results [8], by placing the electronic ground state at 27.05 eV, are shown by vertical lines in the upper part of the figure. The present differential spectrum is similar to the one derived from the data [10], thus indicating the reliability of the analytical photoion spectroscopy. Fig. 2 shows an interesting behavior for the production of the CS_2^{2+} ion, i.e.,

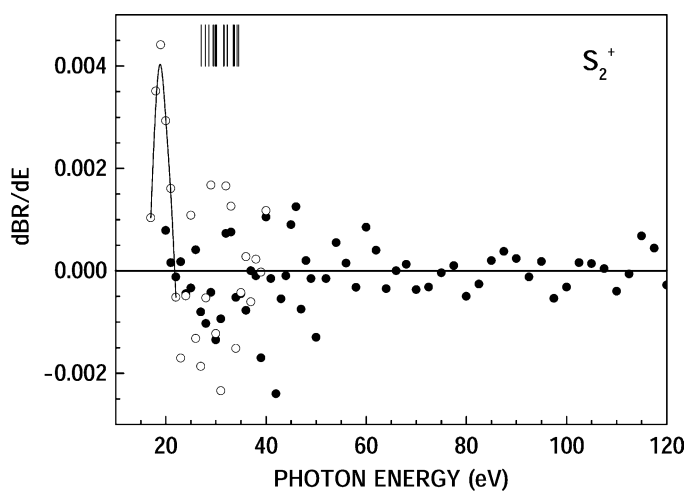

Fig. 6. Differential spectrum of ion branching ratio for S_2^+: (●), present data; (○) and thin solid curve, derived from [10].

the dication is formed only in a narrow energy region from 27.05 to about 35 ± 1 eV (the mean of the present value, ∼36 eV, and the one, ∼34 eV, derived from the data [10]) with a peak at 29 eV. Hochlaf et al. [8] have reported the potential energy curves along the SC–S coordinate for 14 electronic states of CS_2^{2+} using a complete active space self-consistent field (CASSCF) approach and have shown that all low-lying electronic states of CS_2^{2+} are separated by large barriers from their asymptotes. They have further mentioned that all electronic states up to 32–33 eV have bound parts on their potential curves and are stable with respect to dissociation. The present observation may essentially be in agreement with their calculations because there are still some electronic states having shallow bound parts on their potential curves around 35 eV as shown in Fig. 6 [8]. However, the spectral broadening in the present spectroscopy mentioned above should be considered, and yet another possibility may remain that the upper limit at 35 ± 1 eV for the production of the metastable CS_2^{2+} ion is as high as 2–3 eV because the cross section for the production of CS_2^{2+} reported by Lablanquie et al. [9] has a maximum at 32 eV. This issue should be clarified by TPEPICO spectroscopy.

3.3. The CS^+ ion

The first peak in the photoion spectrum derived from the data [10] indicates that the C state dissociates into CS^+ (and also into S^+) of which threshold is at 15.8 eV [19] (Fig. 3). The upper limit of the first peak lies at ∼23.5 eV, which covers the satellite bands 2–9 [2,27], indicating that the lower satellite bands dissociate into CS^+. The second peak is located in the double ionization region. The reported threshold is at 30.2 ± 0.4 eV [9]. This result indicates that the CS^+ ions are formed by the charge separation $S^+ + CS^+$ of the dication. It is interesting to note that the $S^+ + CS^+$ channel is effectively open only in the restricted energy region from ∼30 to ∼42 eV. However, it should also be noted that the upper limit of the energy region is not necessarily definite because whether the ion branching ratio for a given fragment increases or decreases is due to a balance of the ion branching ratios of some fragments. Therefore, it is more appropriate to say that the $S^+ + CS^+$ channel is effectively open at least up to ∼42 eV. Although this matter would be applied to the differential spectra of other fragment ions, it is not repeated in the rest of the paper.

3.4. The C^+ ion

The first peak (∼20 to ∼31.5 eV) covers the satellite bands 4–16 [27], which indicates that these bands dissociate into C^+ (Fig. 4). Aitchison and Eland [3] pointed out that the satellite 4 (19.8–20.5 eV) is the first band from which the production of C^+ is possible. This agrees with the present result. Roy et al. [27] have suggested that the bands with binding energies above 27 eV originate from direct double ionization continua because (1) above 27 eV, no configuration interaction states of CS_2^+ are predicted with significant intensity by ab initio SCF-CI calculations of CS_2^+ corrected for transition moments; and (2) the partial cross section for high lying bands above 27 eV shows a bell shape in close resemblance to the double ionization cross section. However, recent many-body Green's function calculations [2] show discernible intensities of the satellite bands up to 38 eV. It should be noted that the present result (the first peak) can be explained only by the dissociation of these satellite bands, including those in the region of double ionization because the production of C^+ from dissociative double ionization is only possible above 41.5 ± 0.5 eV [9] by the $S^+ + C^+ + S$ dissociation channel of CS_2^{2+} as indicated in the reaction path (3). This implies that the satellite bands in the region of double ionization, at least up to ∼31.5 eV, are valence satellites and are not due to direct double ionization. The second small peak around 35 eV is probably not real from a view that the peak intensity is comparable with the fluctuation of the differential spectrum above 60 eV where the spectrum must be essentially flat. The third peak (∼41 to ∼57 eV) is probably due to the $S^+ + C^+ + S$ channel as mentioned above. It is again interesting to note that the $S^+ + C^+ + S$ channel is effectively open in the restricted region.

3.5. The S^+ ion

The first peak in the differential spectrum derived from the data [10] shows that the C state dissociates into S^+ (as well as CS^+ in Fig. 3) (Fig. 5). The threshold of the production of S^+ is at 14.8 eV [28]. This peak also covers the satellites 1′, 1, and 2 [2,27] on the energy ground. The second peak (the thick solid curve) is broad spreading over ∼20 to ∼48 eV with some structures. The lower part of the second peak from ∼20 to 30.2 eV (the threshold of $S^+ + CS^+$) is probably due to dissociation of the satellite bands 4–15 [27] based on energy considerations. The thin solid curve suggests that dissociation of the satellite 3 is also included although the energy resolution may not be enough to confirm this. The thresholds of the three dissociation channels of CS_2^{2+} [9] are given in the figure. Because of the low energy resolution and counting statistics of the present data, it is difficult to find good correspondence between these thresholds and the rising parts of the structures. A question may arise why the upper limit of the second peak is at ∼48 eV in spite of the observation that the $S^+ + C^+ + S$ channel is open in the region of ∼41 to ∼57 eV (Fig. 4). Above the threshold of $S^+ + C^+ + S$ at 41.5 eV, the three dissociation channels of CS_2^{2+} contribute to the production of S^+ as indicated in the reaction path (3). However, it can be seen that the spectrum for CS^+ (Fig. 3) shows a negative peak in the ∼42 to ∼64 eV region. That is, the upper limit of the second peak is lowered because of the superposition of the negative peak observed in the CS^+ spectrum. This is another limitation of the present spectroscopy.

3.6. The S_2^+ ion

The first peak in the spectrum derived from [10] covers the energy region of ∼17 to ∼21.5 eV, which corresponds to the satellites 2–5 (Fig. 6). This indicates that these satellites dissociate into S_2^+ of which threshold is at 16.9 eV [19]. The production of S_2^+ is interesting because it apparently requires a molecular rearrangement, which occurs only in the narrow energy region. Above ∼21.5 eV, the differential values are scattered because of the weak production of S_2^+ and its poor counting statistics, and nothing can be known above this energy.

4. Conclusion

Ion branching ratios for the molecular and dissociative photoionization of CS_2 have been measured with good accuracy by using time-of-flight mass spectrometry together with synchrotron radiation. The measurements extend to higher photon energy (120 eV) than the previous experiment [10]. The ion branching ratio for the parent CS_2^+ ion increases slightly in the region of 47–80 eV, indicating that electronic states contributing to the production of CS_2^+ exist in this energy region. As for the production of CS_2^+ in the high energy region, it is suggested that double Rydberg states converging to high-lying states of CS_2^{2+} would play an important role. Differentiation of the yield spectra for the observed ions, S_2^+, CS^+, S^+, C^+, and CS_2^{2+}, with respect to the incident photon energy shows, for example, that the $S^+ + CS^+$ dissociation channel of CS_2^{2+} is open in the energy region of 30.2 to ∼42 eV, that the $S^+ + C^+ + S$ dissociation channel is open in the energy region of 41.5 to ∼57 eV, and that the metastable CS_2^{2+} ion is produced in the energy region of 27.05–35 ± 1 eV. Dissociation of satellite bands has also been elucidated.

Acknowledgements

Sincere gratitude is extended to the UVSOR personnel for their assistance during the experiments. This work was supported by the UVSOR Joint Research Program of the Institute for Molecular Science.

References

[1] D. Mathur, F.M. Harris, Mass Spectrom. Rev. 8 (1989) 269, and references therein.
[2] P. Baltzer, B. Wannberg, M. Lundqvist, L. Karlsson, D.M.P. Holland, M.A. MacDonald, M.A. Hayes, P. Tomasello, W. von Niessen, Chem. Phys. 202 (1996) 185.
[3] D. Aitchison, J.H.D. Eland, Chem. Phys. 263 (2001) 449.

[4] S.D. Price, J. Phys. B 25 (1992) 3631.
[5] M. Hochlaf, R.I. Hall, F. Penent, J.H.D. Eland, P. Lablanquie, Chem. Phys. 234 (1998) 249.
[6] T.A. Field, J.H.D. Eland, Chem. Phys. Lett. 303 (1999) 144.
[7] S. Hsieh, J.H.D. Eland, J. Phys. B 30 (1997) 4515.
[8] M. Hochlaf, G. Chambaud, P. Rosmus, J. Chem. Phys. 108 (1998) 4047.
[9] P. Lablanquie, I. Nenner, P. Millie, P. Morin, J.H.D. Eland, M.J. Hubin-Franskin, J. Delwiche, J. Chem. Phys. 82 (1985) 2951.
[10] F. Carnovale, A.P. Hitchcock, J.P.D. Cook, C.E. Brion, Chem. Phys. 66 (1982) 249.
[11] T. Masuoka, T. Horigome, I. Koyano, Rev. Sci. Instrum. 60 (1989) 2179.
[12] T. Masuoka, I. Koyano, J. Chem. Phys. 95 (1991) 909.
[13] T. Masuoka, I. Koyano, N. Saito, Phys. Rev. A 44 (1991) 4309.
[14] T. Masuoka, E. Nakamura, Phys. Rev. A 48 (1993) 4379.
[15] D.M.P. Holland, K. Codling, J.B. West, G.V. Marr, J. Phys. B 12 (1979) 2465.
[16] M.R. Bruce, R.A. Bonham, Z. Phys. D 24 (1992) 149.
[17] C. Ma, C.R. Sporleder, R.A. Bonham, Rev. Sci. Instrum. 62 (1991) 909.
[18] T. Masuoka, A. Okaji, A. Kobayashi, Int. J. Mass Spectrom. 218 (2002) 11.
[19] B. Brehm, J.H.D. Eland, R. Frey, A. Küstler, Int. J. Mass Spectrom. Ion Phys. 12 (1973) 213.
[20] T. Masuoka, J. Chem. Phys. 81 (1984) 2652.
[21] T. Masuoka, S. Mitani, J. Chem. Phys. 90 (1989) 2651.
[22] T. Masuoka, Y. Chung, E.-M. Lee, J.A.R. Samson, J. Chem. Phys. 109 (1998) 2246.
[23] T. Masuoka, A. Kobayashi, J. Chem. Phys. 113 (2000) 1559.
[24] T. Masuoka, Phys. Rev. A 50 (1994) 3886.
[25] T. Masuoka, J. Chem. Phys. 115 (2001) 264.
[26] P. Millie, I. Nenner, P. Archirel, P. Lablanquie, P. Fournier, J.H.D. Eland, J. Chem. Phys. 84 (1986) 1259.
[27] P. Roy, I. Nenner, P. Millié, P. Morin, D. Roy, J. Chem. Phys. 87 (1987) 2536.
[28] V.H. Dibeler, J.A. Walker, J. Opt. Soc. Am. 57 (1967) 1007.